Nonmuscle Myosin Heavy Chain IIA Mutation Predicts Severity and Progression of Sensorineural Hearing Loss in Patients With *MYH9*-Related Disease

Eva J. J. Verver,[1,2] Vedat Topsakal,[1,2] Henricus P. M. Kunst,[3,4] Patrick L. M. Huygen,[3,4] Paula G. Heller,[5] Nuria Pujol-Moix,[6] Anna Savoia,[7] Marco Benazzo,[8] Tiziana Fierro,[9] Wilko Grolman,[1,2] Paolo Gresele,[9] and Alessandro Pecci[10]

Objectives: *MYH9*-related disease (*MYH9*-RD) is an autosomal-dominant disorder deriving from mutations in *MYH9*, the gene for the nonmuscle myosin heavy chain (NMMHC)-IIA. *MYH9*-RD has a complex phenotype including congenital features, such as thrombocytopenia, and noncongenital manifestations, namely sensorineural hearing loss (SNHL), nephropathy, cataract, and liver abnormalities. The disease is caused by a limited number of mutations affecting different regions of the NMMHC-IIA protein. SNHL is the most frequent noncongenital manifestation of *MYH9*-RD. However, only scarce and anecdotal information is currently available about the clinical and audiometric features of SNHL of *MYH9*-RD subjects. The objective of this study was to investigate the severity and propensity for progression of SNHL in a large series of *MYH9*-RD patients in relation to the causative NMMHC-IIA mutations.

Design: This study included the consecutive patients diagnosed with *MYH9*-RD between July 2007 and March 2012 at four participating institutions. A total of 115 audiograms were analyzed from 63 patients belonging to 45 unrelated families with different NMMHC-IIA mutations. Cross-sectional analyses of audiograms were performed. Regression analysis was performed, and age-related typical audiograms (ARTAs) were derived to characterize the type of SNHL associated with different mutations.

Results: Severity of SNHL appeared to depend on the specific NMMHC-IIA mutation. Patients carrying substitutions at the residue R702 located in the short functional SH1 helix had the most severe degree of SNHL, whereas patients with the p.E1841K substitution in the coiled-coil region or mutations at the nonhelical tailpiece presented a mild degree of SNHL even at advanced age. The authors also disclosed the effects of different amino acid changes at the same residue: for instance, individuals with the p.R702C mutation had more severe SNHL than those with the p.R702H mutation, and the p.R1165L substitution was associated with a higher degree of hearing loss than the p.R1165C. In general, mild SNHL was associated with a fairly flat audiogram configuration, whereas severe SNHL correlated with downsloping configurations. ARTA plots showed that the most progressive type of SNHL was associated with the p.R702C, the p.R702H, and the p.R1165L substitutions, whereas the p.R1165C mutation correlated with a milder, nonprogressive type of SNHL than the p.R1165L. ARTA for the p.E1841K mutation demonstrated a mild degree of SNHL with only mild progression, whereas the ARTA for the mutations at the nonhelical tailpiece did not show any substantial progression.

Conclusions: These data provide useful tools to predict the progression and the expected degree of severity of SNHL in individual *MYH9*-RD patients, which is especially relevant in young patients. Consequences in clinical practice are important not only for appropriate patient counseling but also for development of customized, genotype-driven clinical management. The authors recently reported that cochlear implantation has a good outcome in *MYH9*-RD patients; thus, stricter follow-up and earlier intervention are recommended for patients with unfavorable genotypes.

Key words: Age-related typical audiogram, Genotype–phenotype, *MYH9*-related disease, Nonmuscle myosin, Sensorineural hearing loss, Syndromic deafness, Thrombocytopenia.

(Ear & Hearing 2015;XX;00–00)

INTRODUCTION

MYH9-related disease (*MYH9*-RD) is a rare autosomal-dominant syndromic disorder deriving from mutations in *MYH9*, the gene for the nonmuscle myosin heavy chain (NMMHC)-IIA (Kelley et al. 2000; Seri et al. 2000; Balduini et al. 2011). Patients with *MYH9*-RD present with macrothrombocytopenia and characteristic inclusions of the mutant protein in leukocytes since birth. The degree of thrombocytopenia and bleeding tendency is variable among different subjects. During infancy or adult life, most of them develop additional noncongenital manifestations, namely sensorineural hearing loss (SNHL), nephropathy, presenile cataract, and/or alterations of liver enzymes (Balduini et al. 2011; Pecci et al. 2012). *MYH9*-RD encompasses four syndromes that have been considered for many years as distinct disorders, May–Hegglin anomaly (MIM 155100), Sebastian syndrome (MIM 605249), Fechtner syndrome (MIM 153640), and Epstein syndrome (MIM 153650). After the identification of *MYH9* as the gene responsible for all of these disorders, analyses of large series of patients demonstrated that May–Hegglin anomaly, Sebastian, Fechtner, and Epstein syndrome actually represented some of the different possible clinical presentations of the same condition, for which the definition of *MYH9*-RD has been introduced (Seri et al. 2003; Althaus & Greinacher 2010; Kunishima & Saito 2010). The estimated prevalence of *MYH9*-RD is around 1/400,000 although the actual prevalence is expected to be higher since this disorder is still underdiagnosed (Savoia

[1]Department of Otorhinolaryngology and Head and Neck Surgery, University Medical Center Utrecht, Utrecht, The Netherlands; [2]Brain Center Rudolf Magnus, University Medical Center Utrecht, Utrecht, The Netherlands; [3]Department of Otorhinolaryngology, Head and Neck Surgery, Radboud University Medical Centre, Nijmegen, The Netherlands; [4]Donders Institute for Brain, Cognition and Behavior, Radboud University Medical Centre, Nijmegen, The Netherlands; [5]Department of Hematology Research, Instituto de Investigaciones Médicas Alfredo Lanari, UE IDIM-CONICET, University of Buenos Aires, Buenos Aires, Argentina; [6]Institut d'Investigació Biomèdica Sant Pau, Universitat Autònoma de Barcelona, Barcelona, Spain; [7]Institute for Maternal and Child Health, IRCCS "Burlo Garofolo," Trieste, Italy; [8]Department of Otorhinolaryngology, IRCCS Policlinico San Matteo Foundation, Pavia, Italy; [9]Department of Internal Medicine, Section of Internal and Cardiovascular Medicine, University of Perugia, Perugia, Italy; and [10]Department of Internal Medicine, IRCCS Policlinico San Matteo Foundation and University of Pavia, Piazzale Golgi, Pavia, Italy.

<zdoi; 10.1097/AUD.0000000000000198>

& Balduini 2008). To date, more than 300 *MYH9*-RD pedigrees have been reported worldwide (Balduini et al. 2011; Pecci et al. 2014a; Saposnik et al. 2014).

SNHL is the most frequent noncongenital manifestation of *MYH9*-RD: a recent study showed that SNHL was present in about 50% of patients at a mean evaluation age of 35 years and was expected to develop over time in almost all cases (Pecci et al. 2014a). Sporadic observations on small case series suggest a high degree of variability in the severity and propensity for progression of the SNHL among different *MYH9*-RD patients. In fact, some subjects presented with a progressive SNHL leading to profound deafness before the age of 40, whereas other individuals had comparatively stable disease with mild SNHL even at an advanced age (Sekine et al. 2010; De Rocco et al. 2013).

Nonmuscle myosin-IIA is a cytoplasmic myosin participating in several processes requiring generation of chemomechanical forces by the cytoskeleton, such as cell motility, cytokinesis, and maintenance of cell shape (Vicente-Manzanares et al. 2009). It is expressed in most cell types and tissues, including some structures of the inner ear, such as the organ of Corti, spiral ligament, and spiral limbus (Lalwani et al. 2000; Mhatre et al. 2004).

As all conventional myosins, myosin IIA presents a hexameric structure formed by a heavy chain (NMMHC-IIA) dimer and two pairs of light chains. Each NMMHC-IIA molecule comprises two distinct domains: the amino-terminal head domain and the carboxy-terminal tail domain (Eddinger & Meer 2007). The head domain has a globular three-dimensional structure and contains the highly conserved functional regions essential for actin binding, ATPase activity, and generation of the chemomechanical forces (Sellers 2000; Sweeney & Houdusse 2010). The tail domain comprises a long alpha-helical coiled-coil and a short carboxy-terminal nonhelical tailpiece (NHT) (Eddinger & Meer 2007) (Fig. 1A). The coiled-coil is responsible for formation of heavy chain dimers and myosin assembly in functional filaments, whereas the NHT is a phosphorylation site with regulatory functions (Eddinger & Meer 2007; Sanborn et al. 2011).

MYH9-RD is caused by a limited spectrum of *MYH9* mutations that affect different regions of the NMMHC-IIA protein (Balduini et al. 2011). Mutations affect either the head or the tail domain. Almost all mutations in the head domain are point substitutions hitting one of two specific regions of the globular head: a distinct hydrophobic interface between the SH3-like motif and the motor domain (SH3/MD interface) or the arginine at residue 702 (R702) located in the short functional SH1 helix (Fig. 1A) (Kahr et al. 2009; Pecci et al. 2014a). Mutations in the tail domain affect either the coiled-coil or the NHT. The coiled-coil mutations mainly consist of point substitutions, even if in rare pedigrees short in-frame deletions or duplications have been identified. Importantly, three coiled-coil residues are most frequently affected: R1165, D1424, and E1841 (Fig. 1A). Finally, all the mutations affecting the NHT are nonsense or frameshift

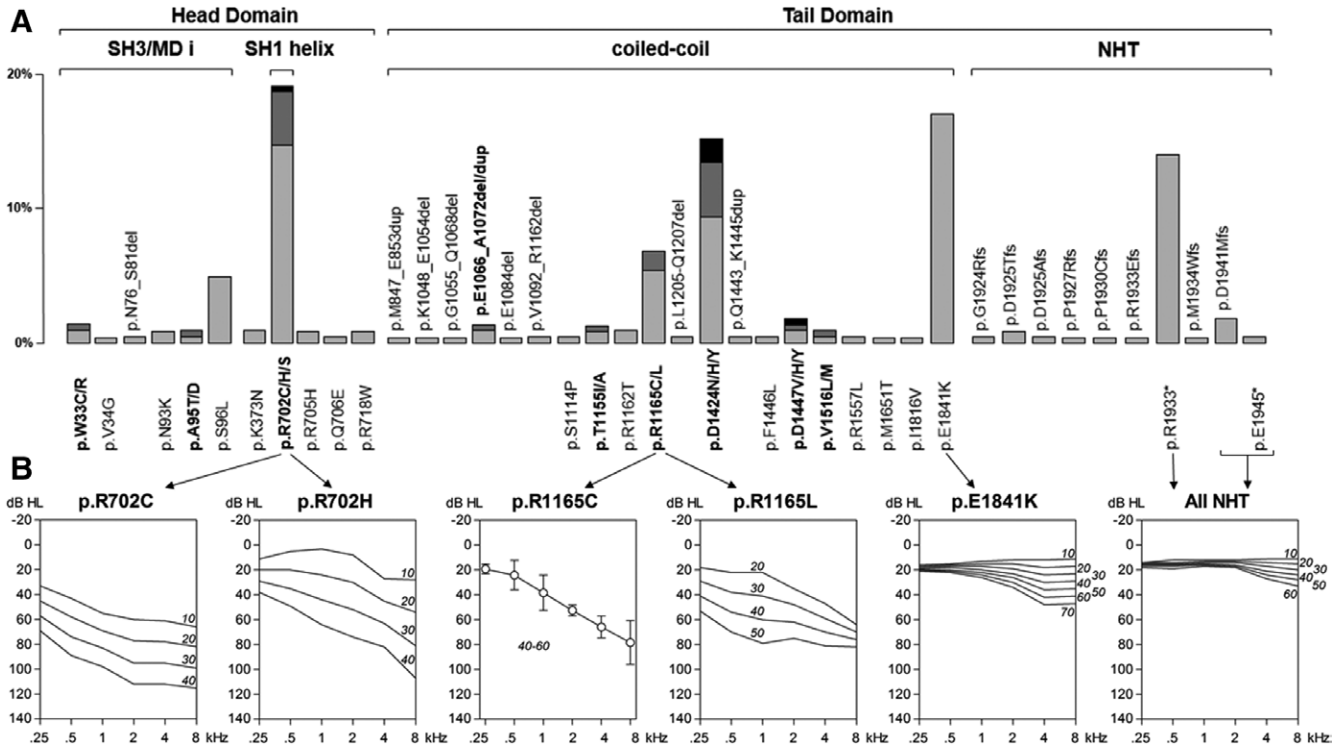

Fig. 1. Spectrum of nonmuscle myosin heavy chain (NMMHC)-IIA mutations identified in the *MYH9*-related disease pedigrees so far. A, NMMHC-IIA mutations are shown together with their relative frequency, which is indicated by the bars' height, and their localization along the different domains (head or tail domain) and regions (SH3-like motif/motor domain interface [SH3/MD i], SH1 helix, coiled-coil, and nonhelical tailpiece [NHT]) of the NMMHC-IIA protein. Missense and nonsense mutations are represented below the bars, while in frame deletions or duplications, frameshift alterations are represented above the bars. The residues indicated in bold are those hit by more than one mutation. Scale on the y axis indicates the relative frequency of the different mutations in the *MYH9*-related disease pedigrees reported so far. B, Age-related typical audiograms for some selected NMMHC-IIA mutations correlated to the schematic representation of the NMMHC-IIA protein. Audiograms at different ages (italics) in decade steps. The p.R1165C panel shows the mean ± 1 SD for threshold in absence of age-dependent progression.

alterations of the last exon (exon 41), resulting in deletion of a variable fragment (13 to 37 residues) of the NHT (Balduini et al. 2011). Previous genotype–phenotype studies showed that patients with mutations in the head domain have a higher risk of developing noncongenital manifestations and more severe thrombocytopenia with respect to patients with mutations affecting the tail domain (Pecci et al. 2008). A more recent investigation also showed that substitutions in the SH1 helix of the head domain were associated with the highest risk of having SNHL and nephropathy, whereas the deletions at the NHT correlated with a significantly lower risk compared to mutations in the other NMMHC-IIA regions (Pecci et al. 2014a).

Given that SNHL is very frequent among *MYH9*-RD patients, an otologist and audiologist are usually involved in clinical management of these patients. However, very scarce and anecdotal data are currently available about the clinical and audiometric features of SNHL of *MYH9*-RD subjects, including descriptions of the severity and rate of progression. To fill this gap, we investigated these features in a large series of *MYH9*-RD patients in relation to their NMMHC-IIA mutations. Age-related typical audiograms (ARTAs) were constructed to characterize the progression of SNHL associated with different genotypes. These data provide essential tools to predict the evolution of the SNHL in individual *MYH9*-RD subjects and therefore contribute to the opportunity to offer more personalized patient care.

MATERIALS AND METHODS

Patients

This study included all the consecutive patients diagnosed with *MYH9*-RD between July 2007 and March 2012 at four different participating institutions for whom audiograms were available. All the audiograms available for each patient were collected and retrospectively analyzed. Audiometric examinations were performed between June 1992 and July 2013. In all cases, the diagnosis was based on the immunofluorescence assay for the identification of pathognomonic NMMHC-IIA leukocyte aggregates and on the identification of the causative mutation by molecular screening of *MYH9* (Savoia et al. 2010). Both analyses were centralized (Department of Internal Medicine, IRCCS Policlinico San Matteo Foundation, Pavia, Italy, and Institute for Maternal and Child Health, IRCCS Burlo Garofolo, Trieste, Italy, respectively) and were carried out as previously described (Savoia et al. 2010). All the patients and mutations have been previously reported (Pecci et al. 2014a). All patients or their legal guardians provided written informed consent. The investigation was approved by the Institutional Review Board of the IRCCS Policlinico San Matteo Foundation.

Audiometric Examination

Pure-tone audiometry was performed at each referring institution according to current clinical standards to determine hearing thresholds at least at six frequencies (0.25, 0.5, 1, 2, 4, and 8 kHz). The binaural mean air conduction (AC) threshold at any given audio frequency was included in the data analysis only if the mean air-bone gap (ABG) averaged for 0.5 to 2 kHz was 15 dB or less and if the thresholds were fairly symmetric. A difference between left and right ear AC threshold of >20 dB for at least three consecutive frequencies was labeled as asymmetric SNHL. When an ear was excluded from analysis because of an intolerable asymmetry or an ABG in excess of 15 dB, pure-tone thresholds from the better ear was used instead of the binaural mean threshold.

Statistical Testing for Hearing Impairment Beyond ISO 7029 Estimates of Presbyacusis

Hearing is known to deteriorate with age (presbyacusis). Hearing impairment develops more rapidly at high than at low frequencies, and men are more severely affected than women. However, the effect of age-related hearing impairment varies considerably among individuals. Furthermore, a decrease in hearing ability may not necessarily be caused by aging itself but may also be influenced by environmental as well as genetic factors. The ISO 7029 (International Organization for Standardization, ISO 7029 1984) established the expected pure-tone hearing thresholds distributions of otologically normal subjects aged between 18 and 70 years who have not been exposed to known risk factors for hearing impairment. Apart from median (P50) values by age and gender, ISO 7029 also specifies several percentiles: P75, P90, and P95, or the percentiles 75, 90, and 95, that is, the 75%, 90%, and 95% tail probabilities, respectively, for the sample distribution at a given age to characterize the variability in hearing impairment that results from presbyacusis. These data can be used to estimate the amount of hearing impairment caused by a specific agent or genetic factor in a population. In this study of patients with *MYH9*-RD, pure-tone thresholds were compared to the age- and gender-related distributions as defined by the ISO 7029 standard. Thus, for each frequency, the threshold can be expressed as beyond the P95, P90, P75, or P50 of the age- and gender-dependent control curve of the general population.

For each ear, four tests were performed to determine whether there was significant hearing impairment beyond presbyacusis and if it was beyond the P95, P90, P75, or P50 of ISO 7029 estimates of presbyacusis (ISO 7029). Hearing impairment in a given ear was considered to represent impairment beyond estimates of presbyacusis if two of six (2/6) (or more) audiometric frequencies had a threshold beyond the P95, three of six (or more) beyond the P90, four of six (or more) beyond the P75, or six of six beyond the P50 of ISO 7029 estimates of presbyacusis. When the P95 criterion was fulfilled, hearing impairment in that ear was considered to be present beyond the P95 level of presbyacusis. When the P95 test failed but the P90 test was positive, hearing impairment was considered to be present beyond the P90 level of presbyacusis, etc. When the P50 test failed, it was concluded that there was no significant hearing impairment beyond presbyacusis.

Regression Analysis and ARTAs

Binaural mean AC thresholds (dB HL), obtained from the last-visit audiogram of each patient, were plotted against age for each frequency. A commercial program, Prism version 3.0 (Graph-Pad, San Diego, CA), was used for linear regression analyses (threshold on age). The regression coefficient, that is, the slope, was called annual threshold deterioration (ATD, in decibels per year). We evaluated the significance of hearing loss progression at each frequency; this required that the 95% confidence interval for the regression coefficient, or the ATD, did not include zero. Hearing impairment was labeled as progressive when two or more of six frequencies showed significant

progression ($p = 0.0088$ according to the binomial distribution with N = 6, $p = 0.025$, $q = 0.075$).

Based on the regression analysis, ARTAs were constructed, which show the predicted thresholds for a number of decade steps in age (Huygen et al. 2003). Results of the linear regression analysis of the group cross-sectional last-visit data were compared with those of the linear regressions of the available individual longitudinal thresholds from serial audiograms to ensure that there was general agreement.

RESULTS

Patients

We obtained 123 audiometric examinations of 65 patients with *MYH9*-RD belonging to 47 unrelated families. Because of asymmetric hearing loss (11 ears), ABG (17 ears), both asymmetric hearing loss and ABG (2 ears), or incomplete hearing assessments (6 ears), data from one ear (n = 20) and both ears (n = 8) were excluded. Therefore, our data analysis included 115 audiometric examinations of 63 patients from 45 families. There were 25 males and 38 females with a mean age at the time of the last audiometric examination of 33.8 years (range, 4 to 72). Table 1 details the genotypic features of the investigated subjects.

Cross-Sectional Analyses of Audiograms

The obtained audiograms are shown in Figure 2. Each panel of Figure 2 combines the last-visit audiograms (binaural mean AC threshold in dB HL) for the subjects specified in the panel title. Patients were grouped in each panel according to the specific NMMHC-IIA mutation, and panels were clustered according to the NMMHC-IIA region affected by mutation (SH3/MD interface, SH1 helix, coiled-coil, or NHT, see Table 1). For example, the bottom right panel shows these audiograms obtained from patients 14, 15, and 52, all carrying the p.E1945* mutation located in the NHT at the ages of 30.07, 34.38, and 56.75 years, respectively.

Hearing Impairment Beyond ISO 7029 Standards for Age-Related Hearing Loss

All the investigated patients showed significant hearing impairment beyond the P95, P90, P75, or P50 estimates of age-related hearing loss (ISO 7029), with the single exception of patient 12, aged 56.68 years, who carried the p.E1841K mutation in the coiled-coil.

Variability in Level of Hearing Impairment Within Subgroups

Much of the variability in the severity of SNHL shown in Figure 2 seemed to depend on age. However, there were some notable exceptions. Among the patients 30, 45, and 46 with the p.D1447V mutation in the coiled-coil, the youngest patient 46 had the poorest threshold at relatively young age (35.45 years), whereas patient 45 had the best threshold at the highest age (66.65 year). Patient 61 with the p.R702C mutation in the SH1 helix had severe SNHL by the age of 13.20 years (Fig. 2). For the cross-sectional analysis discussed below, we evaluated whether this measurement might be interpreted as an outlier, but it appeared that this measurement fitted within the 95% and 90% prediction bands for the regression line (threshold on age) at each frequency. The two top-right panels in Figure 2 demonstrate that a distinctive feature of the thresholds in the carriers of the p.R702C or p.R702H mutation was the large variability in their degree of SNHL, which could be associated with wide prediction bands for the associated cross-sectional regression

TABLE 1. Genotypic features of 63 investigated patients with *MYH9*-related disease

MYH9 Exon	*MYH9* Mutation*	NMMHC-IIA Domain	NMMHC-IIA Region	NMMHC-IIA Mutation	No. Patients (No. Families)	No. Audiograms
2	c.101T>G	HD	SH3/MD i	p.V34G	1 (1)	1
2	c.284C>A	HD	SH3/MD i	p.A95D	2 (1)	5
2	c.287C>T	HD	SH3/MD i	p.S96L	2 (1)	2
17	c.2104C>T	HD	SH1 helix	p.R702C	7 (7)	20
17	c.2105G>A	HD	SH1 helix	p.R702H	6 (5)	11
21	c.2539_2559dup	TD	Coiled-coil	p.M847_E853dup	2 (1)	4
25	c.3195_3215dup	TD	Coiled-coil	p.E1066_A1072dup	2 (2)	3
25	c.3195_3215del	TD	Coiled-coil	p.E1066_A1072del	2 (2)	5
26	c.3464C>T	TD	Coiled-coil	p.T1155I	1 (1)	1
27	c.3493C>T	TD	Coiled-coil	p.R1165C	3 (2)	8
27	c.3494G>T	TD	Coiled-coil	p.R1165L	4 (2)	9
31	c.4270G>A	TD	Coiled-coil	p.D1424N	3 (2)	8
31	c.4270G>C	TD	Coiled-coil	p.D1424H	2 (2)	8
31	c.4270G>T	TD	Coiled-coil	p.D1424Y	2 (2)	5
31	c.4340A>T	TD	Coiled-coil	p.D1447V	3 (2)	4
32	c.4546G>A	TD	Coiled-coil	p.V1516M	1 (1)	1
33	c.4670G>T	TD	Coiled-coil	p.R1557L	1 (1)	1
39	c.5521G>A	TD	Coiled-coil	p.E1841K	5(3)	13
41	c.5797C>T	TD	NHT	p.R1933*	9 (5)	9
41	c.5821delG	TD	NHT	p.D1941Mfs*7	2 (1)	2
41	c.5833G>T	TD	NHT	p.E1945*	3 (1)	3
Total					63 (45)	115

**Nucleotide numbering reflects the MYH9 complementary DNA with +1 corresponding to the A of the ATG translation initiation codon in the reference sequence (RefSeq NM_002473.4). The initiation codon is codon 1.*

HD, head domain; NHT, nonhelical tailpiece; NMMHC, nonmuscle myosin heavy chain; SH3/MD I, SH3-like motif/motor domain interface; TD, tail domain.

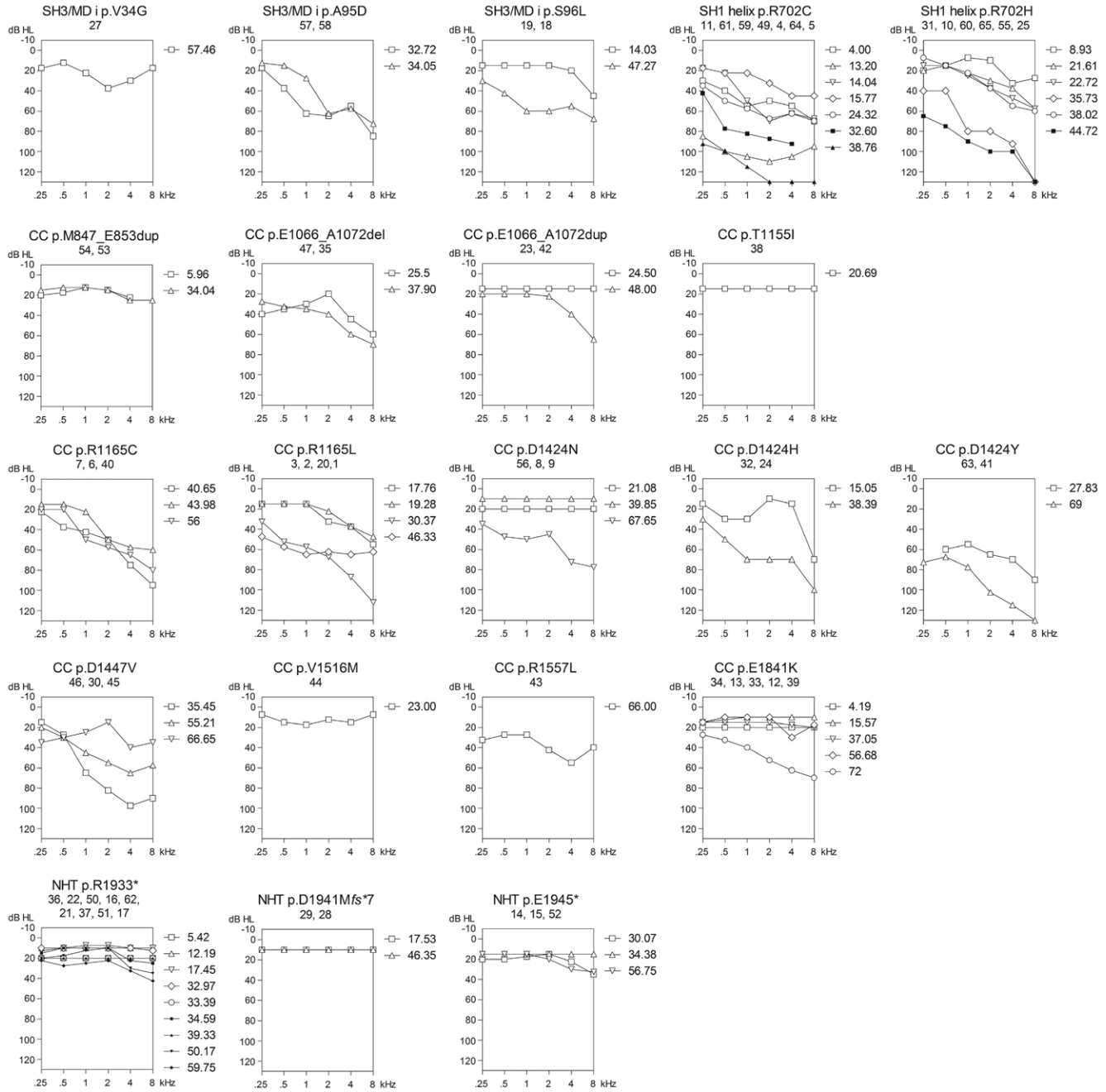

Fig. 2. All last-visit audiograms (binaural mean air conduction threshold in dB HL plotted against frequency in kHz) obtained for the various subgroups of patients with different mutations. The panel titles indicate the nonmuscle myosin heavy chain (NMMHC)-IIA region, mutation, and the individual ID numbers of the individuals covered. Panels were clustered according to the NMMHC-IIA region affected by mutation (SH3-like motif/motor domain interface [SH3/MD i], SH1 helix, coiled-coil [CC], or nonhelical tailpiece [NHT]). The key to each panel specifies the individual's age at the last-visit audiometry (in years) in the same order (top to bottom) as the individual ID numbers (left to right) in the panel title.

lines if a substantial part of this variability was not strictly age-dependent. Indeed, a lack of significant progression found in the cross-sectional analysis of the thresholds in the p.R702C carriers (see below, Fig. 4) was an associated finding.

Hearing Impairment Evaluated by Progression, Cross-Sectional Analyses

Figure 3A shows all the available threshold data in a mixed single-snapshot plot, that is, individual longitudinal data mixed with cross-sectional last-visit data, for the mutations in the SH1 helix, p.R702C and p.R702H. This plot suggests that hearing in patients with the p.R702C substitution is more severely affected than those with the p.R702H. In fact, in the plots for 0.5 to 4 kHz (Fig. 3A only shows 1-kHz plot as example), it is possible to divide the plotting area into an (irregularly shaped) upper/left part and a lower/right part in such a way that the upper/left part includes only the seven p.R702C patients and the lower/right part includes only the six p.R702H patients. These counts, when tested in a 2×2 table using Fisher exact

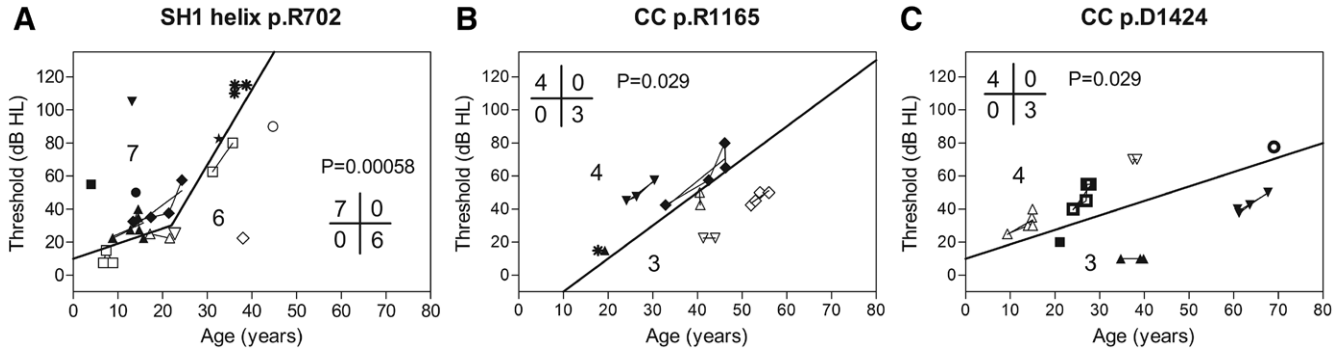

Fig. 3. Mixed single snapshot for the SH1 helix R702 mutation (A), coiled-coil (CC) R1165 mutation (B), and coiled-coil D1424 mutation (C). For each mutation, only the thresholds at 1 kHz are shown as an example. Threshold in dB HL plotted against age in years. In each plot, data points for each individual are shown by a different symbol. Consecutive thresholds for one and the same person are connected by lines. Different mutations are indicated by different types of symbols (solid/open/bold) (see below for symbol keys). Dividing lines are shown with the number of patients counted on each side of the line. The inset shows the corresponding 2 × 2 table and the *p* value for the associated Fisher exact test. Keys to symbols: (A) solid symbols p.R702C, open symbols p.R702H; (B) solid symbols p.R1165L, open symbols p.R1165C; (C) solid symbols p.D1424N, open symbols p.D1424H, open bold symbols p.D1424Y.

test, disclosed significantly different distributions of the data points pertaining to these two different mutations ($p = 0.00058$, inset in plot). Similarly, the upper/left part in the 8-kHz panel includes the seven p.R702C patients and one p.R702H patient, and the lower/right part includes five p.R702H subjects (data not shown). These counts were also associated with significantly different data point distributions pertaining to these two mutations ($p = 0.0045$).

Figure 4 shows the regression analyses of the cross-sectional threshold data for the p.R702C/H mutations. The plots for patients with the p.R702C mutation as well as for those with the p.R702H shown in Figures 3A and 4 are suggestive of progression. However, ATD reached statistical significance only for the patients with the p.R702H mutation at 2 to 8 kHz, by 1.8 to 2.6 dB/year.

We created mixed single-snapshots plots also for the coiled-coil mutations p.R1165C and p.R1165L. At 0.25 to 1 kHz, it was possible to divide the plotting area into an upper/left part (associated with higher thresholds at predominantly younger ages) and a lower/right part (associated with lower thresholds at predominantly more advanced ages) in such a way that the upper/left part includes only the four p.R1165L patients and the lower/right part includes only the three p.R1165C patients (Fig. 3B only shows 1-kHz plot as example). These counts resulted in a significantly different distribution ($p = 0.029$), suggesting that SNHL is more severe in patients carrying the p.R1165L mutation than in patients with the p.R1165C. The p.R1165L substitution was associated with significant progression (last-visit data only in cross-sectional analysis) at 0.25 to 1 kHz by 1.2 to 1.8 dB/year (regression data not shown).

Concerning the mutations affecting the D1424 residue, mixed single-snapshot plots for 1 to 8 kHz suggested that the hearing levels in p.D1424Y patients are fairly in line with those in p.D1424H patients, at levels that are worse than found in the p.D1424N patients, possibly by 30 dB or more at any age. In fact, it was possible to divide the plotting area of the panels for 0.5 to 8 kHz (Fig. 3C only shows 1 kHz as example) into an upper/left part that includes only the four p.D1424H or p.D1424Y patients and a lower/right part that includes only the three p.D1424N patients. These counts also disclosed significantly different distributions ($p = 0.029$). SNHL was therefore more severe in patients carrying the p.D1424H or p.D1424Y mutation than in patients carrying the p.D1424N.

Patients with the NHT mutation p.R1933* showed minimal but significant progression at 4 to 8 kHz by as low as 0.4 to 0.5 dB/year; there was no appreciable progression found among carriers of the p.D1941Mfs* or p.E1945* mutations in the NHT (data not shown).

Age-Related Typical Audiograms

The cross-sectional regression analyses pertaining to only a few domains or mutations were suitable for deriving ARTA.

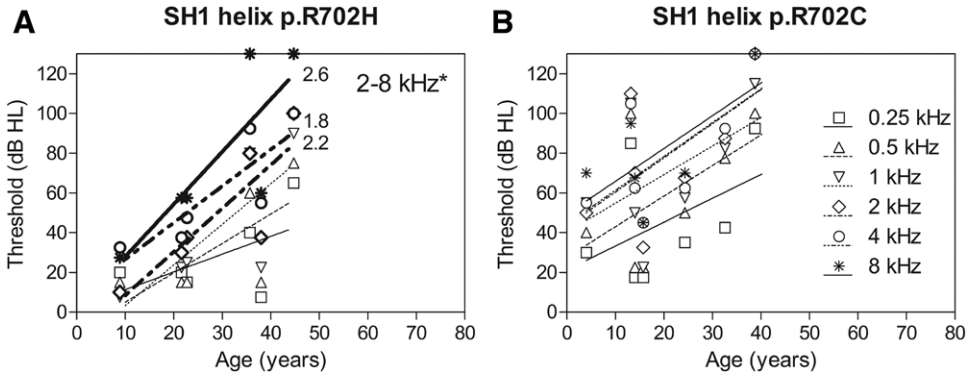

Fig. 4. Cross-sectional analysis of pure-tone thresholds of persons with SH1 helix mutations p.R702H (A) and p.R702C (B). Threshold in dB HL plotted against age in years. Annual threshold deterioration (in dB/yr) is shown for frequencies with significant progression (*) as indicated by bold lines and symbols.

The relevant ARTA is shown in Figure 1B correlated to the schematic representation of the NMMHC-IIA protein. Given the findings illustrated in Figure 3A, B, there is separate ARTA for the SH1 helix p.R702C and p.R702H mutations, as well as for the coiled-coil p.R1165C and p.R1165L mutations. As the threshold data for the p.R1165C patients did not suggest progression, an average, that is, age-independent, audiogram is presented for these patients. Finally, the separate data for the mutations in the NHT region could be combined into a single regression analysis (data not shown).

The ARTA plots show a more severe and progressive SNHL associated with the SH1 helix p.R702C and p.R702H mutations and with the coiled-coil mutation p.R1165L, whereas the p.R1165C mutation appeared to be associated with a milder SNHL than the p.R1165L. The ARTA for the coiled-coil p.E1841K substitution demonstrated very mild levels of SNHL with only mild progression, whereas the NHT mutations had minimal progression (see also Fig. 2).

In general, relatively mild SNHL was associated with a fairly flat audiogram configuration (p.E1841K mutation, all NHT mutations), whereas more severe SNHL was associated with downsloping configurations (p.R702C/H, p.R1165C/L).

Carriers of the SH1 helix p.R702C/H mutations or the coiled-coil p.R1165L mutation suggested progression similar to, or perhaps even beyond, presbyacusis. This is derived from the observation that the average P50 age-related change in hearing sensitivity at 8 kHz for men and women increases by on the order of 5 dB from age 30 to 40 (reference data not shown). Between the same ages, the average P95 increase in age-related hearing sensitivity for men and women is on the order of 10 dB. Figure 1B shows threshold increases between age 30 and age 40 of ~15 dB and ~25 dB for the p.R702C and p.R702H mutations, respectively; for the p.R1165L mutation, a corresponding increase of ~5 dB can be seen at 8 kHz. Given the variability in threshold in these groups of carriers, we did not attempt to perform any statistical test on progression compared to the ISO 7029 norm. Remarkably, the progression shown by the patients with the coiled-coil p.R1165L mutation was more concentrated in the lower frequencies, unlike the pattern of progression that is commonly associated with presbyacusis.

DISCUSSION

MYH9-RD is a syndromic disorder with a complex clinical phenotype, which includes congenital features, such as thrombocytopenia and leukocyte inclusions, and noncongenital manifestations, namely SNHL, kidney damage, cataract, and liver impairment (Kunishima & Saito 2010; Balduini et al. 2011; Pecci et al. 2012). *MYH9*-RD is caused by a limited number of *MYH9* mutations that affect different regions of the NMMHC-IIA protein (Balduini et al. 2011). Previous genotype–phenotype studies investigated the risk of developing the noncongenital manifestations (including SNHL) associated with the specific NMMHC-IIA alterations. An earlier study demonstrated that patients with mutations in the head domain, taken together, have a higher risk of developing SNHL and nephropathy as compared with patients with mutations hitting the tail domain (Pecci et al. 2008). A recent analysis of a larger case series provided a more accurate hierarchical prognostic model, as it disclosed a different risk of developing SNHL deriving from different mutations hitting the same domain, and even the same residue. In particular, this analysis identified three genotype subgroups with significantly different risks: (1) Substitutions at residue R702 (SH1 helix) were associated with a significantly higher prevalence of SNHL; (2) mutations hitting the SH3/MD interface, the p.R1165C/L, and p.D1424H/Y substitutions resulted in an intermediate-high risk; and (3) finally, the p.D1424N and p.E1841K substitutions and NHT mutations correlated with the significantly lower risk of developing SNHL over time (Pecci et al. 2014a).

SNHL is the markedly most frequent noncongenital manifestation of the *MYH9*-RD, as it is expected to develop over time in almost all patients (Pecci et al. 2014a). Notwithstanding this, there is very limited information about the clinical and audiometric features of the SNHL manifested by individuals with *MYH9*-RD, including descriptions of hearing loss severity and progression. Here, we systematically investigated these features in a series of 63 *MYH9*-RD patients with known NMMHC-IIA mutations.

All the investigated patients but one showed significant SNHL beyond the P95, P90, P75, or the P50 derived from the ISO 7029 standard for age-related hearing loss. Concerning the severity of the SNHL, subjects with substitutions affecting the residue R702 in the SH1 helix had the most severe degree of SNHL, while patients with NHT mutations or the p.E1841K mutation in the coiled-coil presented a very mild SNHL even at an advanced age. Moreover, we demonstrated a different effect deriving from different substitutions at the residue D1424, as the p.D1424N substitution was associated with a lower degree of SNHL compared with the p.D1424H or p.D1424Y.

This genotype–phenotype picture is globally consistent with that derived from the previous study evaluating the risk of developing SNHL (Pecci et al. 2014a), indicating that the NMMHC-IIA alterations associated with the higher prevalence of SNHL also result in the higher severity of the SNHL, probably reflecting a higher degree of NMMHC-IIA loss-of-function. However, the present study disclosed novel and important genotype–phenotype correlations that were not identified by previous investigations. In particular, we showed that patients with the p.R702C substitution had more severe SNHL than subjects with the p.R702H substitution, while previous studies reported that the risk of developing SNHL was not different between the p.R702C and p.R702H mutations (Pecci et al. 2014a). This suggests that even if patients with the p.R702C or p.R702H mutation have the same probability of developing a SNHL, the subjects with the p.R702C mutation may develop a more severe degree of SNHL, as compared with individuals carrying the p.R702H mutation. A similar comment can be made for the substitutions at the residue R1165. In fact, we observed that patients with the p.R1165L had a more severe degree of SNHL than patients carrying the p.R1165C, while the relative prevalence of SNHL was similar between these two mutations.

Concerning the audiogram configuration, we showed that, in general, relatively mild SNHL was associated with a fairly flat configuration most common for the coiled-coil p.E1841K mutation and NHT mutations. Instead, more severe SNHL was associated with downsloping configurations as seen in most mutations in the head domain and some mutations in the coiled-coil.

Concerning the progression of SNHL, a few mutations were suitable for constructing ARTA plots. This analysis showed that the most severe and progressive SNHL was associated with the

SH1 helix mutations and with the mutation p.R1165L, whereas the p.R1165C mutation appeared to be associated with a milder, nonprogressive SNHL compared with the p.R1165L mutation. The ARTA for the coiled-coil p.E1841K mutation demonstrated very mild levels of SNHL combined with very mild progression, whereas the ARTA for the NHT mutations, at similar starting levels of SNHL, did not show any substantial progression (Fig. 1).

Altogether, these data provide useful tools to predict the propensity for progression and the expected degree of severity of SNHL in individual *MYH9*-RD patients, especially in young subjects. For example, a patient presenting with SNHL and the p.R702C mutation is expected to experience a rapid deterioration over time leading to a severe SNHL at a relatively young age, compared with a patient with SNHL and a mutation in the NHT, who is expected to have a mild SNHL even at a more advanced age, without substantial deterioration. Consequences in clinical practice are relevant for development of personalized, genotype-driven clinical management. We recently reported that cochlear implantation is effective in restoring hearing function and verbal communication ability in patients with *MYH9*-RD and severe to profound SNHL (Pecci et al. 2014b). We also observed that as with other forms of postlingual SNHL, the duration of deafness before implantation negatively affects cochlear implant performance (Blamey et al. 1996, 2013). Thus, a stricter follow-up and earlier surgery should be considered for patients with unfavorable genotypes, such as substitutions of R702 in the SH1 helix or the p.R1165L mutation in the coiled-coil.

The mechanism by which *MYH9* dysfunction causes SNHL is still unknown. Studies in rodents showed that NMMHC-IIA is expressed in the hair cells of the organ of Corti, spiral ligament and spiral limbus, with only minimal expression within the spiral ganglion (Lalwani et al. 2000; Mhatre et al. 2006). In hair cells, NMMHC-IIA was localized along the length of the stereocilia, the cuticular plate, and the plasma membrane (Mhatre et al. 2006; Lalwani et al. 2008). On this basis, it was hypothesized that *MYH9* mutations cause SNHL by altering the structural integrity of stereocilia, similarly to what has been observed in mouse models of deafness deriving from mutations in three other members of the myosin superfamily, namely myosin VI, VIIA, and XVA (Avraham et al. 1995; Probst et al. 1998; Self et al. 1998; Self et al. 1999; Rzadzinska et al. 2004). Concerning the prominent NMMHC-IIA expression in the spiral ligament, fibrocytes belong to the major cellular components of this connective tissue. These cells are supposed to play a role in providing anchorage for surrounding cells or developing or reacting to tension generated in the basilar membrane–spiral ligament complex (Henson et al. 1984). Mhatre et al. (2006) hypothesized that dysfunction of *MYH9* could contribute to SNHL by disrupting the functions mediated by the fibrocytes of the spiral ligament. Indeed, the observation that cochlear implantation has a good outcome in *MYH9*-RD patients is consistent with these pathogenetic hypotheses, as the cochlear implant directly stimulates the spiral ganglion and thereby bypasses hair cell stereocilia and spiral ligament.

In conclusion, we reported for the first time systematic information on the clinical and audiometric features of SNHL in patients with *MYH9*-RD. We showed that severity and progression of SNHL are largely dependent on the causative NMMHC-IIA mutation, and we provided useful findings for patient counseling and clinical management.

ACKNOWLEDGMENTS

This work was supported in part by a grant from the IRCCS Policlinico San Matteo Foundation (to A.P.).

The authors declare no other conflict of interest.

Address for correspondence: Eva J. J. Verver, Department of Otorhinolaryngology and Head and Neck Surgery, Rudolf Magnus Institute of Neuroscience, University Medical Center Utrecht, P.O. Box 85500, Internal Post Number G05.129, 3508 GA Utrecht, The Netherlands. E-mail: ent-research@umcutrecht.nl

Received August 25, 2014; accepted June 12, 2015.

REFERENCES

Althaus, K., & Greinacher, A. (2010). MYH-9 related platelet disorders: Strategies for management and diagnosis. *Transfus Med Hemother*, *37*, 260–267.

Avraham, K. B., Hasson, T., Steel, K. P., et al. (1995). The mouse Snell's waltzer deafness gene encodes an unconventional myosin required for structural integrity of inner ear hair cells. *Nat Genet*, *11*, 369–375.

Balduini, C. L., Pecci, A., Savoia, A. (2011). Recent advances in the understanding and management of MYH9-related inherited thrombocytopenias. *Br J Haematol*, *154*, 161–174.

Blamey, P., Arndt, P., Bergeron, F., et al. (1996). Factors affecting auditory performance of postlinguistically deaf adults using cochlear implants. *Audiol Neurootol*, *1*, 293–306.

Blamey, P., Artieres, F., Başkent, D., et al. (2013). Factors affecting auditory performance of postlinguistically deaf adults using cochlear implants: An update with 2251 patients. *Audiol Neurootol*, *18*, 36–47.

De Rocco, D., Zieger, B., Platokouki, H., et al. (2013). MYH9-related disease: Five novel mutations expanding the spectrum of causative mutations and confirming genotype/phenotype correlations. *Eur J Med Genet*, *56*, 7–12.

Eddinger, T. J., & Meer, D. P. (2007). Myosin II isoforms in smooth muscle: Heterogeneity and function. *Am J Physiol Cell Physiol*, *293*, C493–C508.

Henson, M. M., Henson, O. W., Jr, Jenkins, D. B. (1984). The attachment of the spiral ligament to the cochlear wall: Anchoring cells and the creation of tension. *Hear Res*, *16*, 231–242.

Huygen, P. L., Pennings, R. J., Cremers, C. W. (2003). Characterizing and distinguishing progressive phenotypes in nonsyndromic autosomal dominant hearing impairment. *Audiol Med*, *1*, 37–46.

International Organization for Standardization, ISO 7029. (1984). *Acoustics—Threshold of Hearing by Air Conduction as a Function of Age and Sex for Otologically Normal Persons*. Geneva, Switzerland.

Kahr, W. H., Savoia, A., Pluthero, F. G., et al. (2009). Megakaryocyte and platelet abnormalities in a patient with a W33C mutation in the conserved SH3-like domain of myosin heavy chain IIA. *Thromb Haemost*, *102*, 1241–1250.

Kelley, M. J., Jawien, W., Ortel, T. L., et al. (2000). Mutation of MYH9, encoding non-muscle myosin heavy chain A, in May-Hegglin anomaly. *Nat Genet*, *26*, 106–108.

Kunishima, S., & Saito, H. (2010). Advances in the understanding of MYH9 disorders. *Curr Opin Hematol*, *17*, 405–410.

Lalwani, A. K., Atkin, G., Li, Y., et al. (2008). Localization in stereocilia, plasma membrane, and mitochondria suggests diverse roles for NMHC-IIa within cochlear hair cells. *Brain Res*, *1197*, 13–22.

Lalwani, A. K., Goldstein, J. A., Kelley, M. J., et al. (2000). Human nonsyndromic hereditary deafness DFNA17 is due to a mutation in nonmuscle myosin MYH9. *Am J Hum Genet*, *67*, 1121–1128.

Mhatre, A. N., Li, J., Kim, Y., et al. (2004). Cloning and developmental expression of nonmuscle myosin IIA (Myh9) in the mammalian inner ear. *J Neurosci Res*, *76*, 296–305.

Mhatre, A. N., Li, Y., Atkin, G., et al. (2006). Expression of Myh9 in the mammalian cochlea: Localization within the stereocilia. *J Neurosci Res*, *84*, 809–818.

Pecci, A., Biino, G., Fierro, T., et al; Italian Registry for MYH9-related diseases. (2012). Alteration of liver enzymes is a feature of the MYH9-related disease syndrome. *PLoS One*, *7*, e35986.

Pecci, A., Klersy, C., Gresele, P., et al. (2014a). MYH9-related disease: A novel prognostic model to predict the clinical evolution of the disease based on genotype-phenotype correlations. *Hum Mutat*, *35*, 236–247.

Pecci, A., Panza, E., Pujol-Moix, N., et al. (2008). Position of nonmuscle myosin heavy chain IIA (NMMHC-IIA) mutations predicts the natural history of MYH9-related disease. *Hum Mutat*, *29*, 409–417.

Pecci, A., Verver, E. J., Schlegel, N., et al. (2014b). Cochlear implantation is safe and effective in patients with MYH9-related disease. *Orphanet J Rare Dis*, *9*, 100.

Probst, F. J., Fridell, R. A., Raphael, Y., et al. (1998). Correction of deafness in shaker-2 mice by an unconventional myosin in a BAC transgene. *Science*, *280*, 1444–1447.

Rzadzinska, A. K., Schneider, M. E., Davies, C., et al. (2004). An actin molecular treadmill and myosins maintain stereocilia functional architecture and self-renewal. *J Cell Biol*, *164*, 887–897.

Sanborn, K. B., Mace, E. M., Rak, G. D., et al. (2011). Phosphorylation of the myosin IIA tailpiece regulates single myosin IIA molecule association with lytic granules to promote NK-cell cytotoxicity. *Blood*, *118*, 5862–5871.

Saposnik, B., Binard, S., Fenneteau, O., et al; French MYH9 network. (2014). Mutation spectrum and genotype-phenotype correlations in a large French cohort of MYH9-Related Disorders. *Mol Genet Genomic Med*, *2*, 297–312.

Savoia, A., & Balduini, C. L. (2008). MYH9-related disorders. In R. A. Pagon, M. P. Adam, H. H. Ardinger, *et al*. (Eds.), *GeneReviews® 2008*. Retrieved April 5, 2011, from https://www.ncbi.nlm.nih.gov/books/NBK2689/.

Savoia, A., De Rocco, D., Panza, E., et al. (2010). Heavy chain myosin 9-related disease (MYH9-RD): Neutrophil inclusions of myosin-9 as a pathognomonic sign of the disorder. *Thromb Haemost*, *103*, 826–832.

Sekine, T., Konno, M., Sasaki, S., et al. (2010). Patients with Epstein-Fechtner syndromes owing to MYH9 R702 mutations develop progressive proteinuric renal disease. *Kidney Int*, *78*, 207–214.

Self, T., Mahony, M., Fleming, J., et al. (1998). Shaker-1 mutations reveal roles for myosin VIIA in both development and function of cochlear hair cells. *Development*, *125*, 557–566.

Self, T., Sobe, T., Copeland, N. G., et al. (1999). Role of myosin VI in the differentiation of cochlear hair cells. *Dev Biol*, *214*, 331–341.

Sellers, J. R. (2000). Myosins: A diverse superfamily. *Biochim Biophys Acta*, *1496*, 3–22.

Seri, M., Cusano, R., Gangarossa, S., et al. (2000). Mutations in MYH9 result in the May-Hegglin anomaly, and Fechtner and Sebastian syndromes. The May-Hegglin/Fechtner Syndrome Consortium. *Nat Genet*, *26*, 103–105.

Seri, M., Pecci, A., Di Bari, F., et al. (2003). MYH9-related disease: May-Hegglin anomaly, Sebastian syndrome, Fechtner syndrome, and Epstein syndrome are not distinct entities but represent a variable expression of a single illness. *Medicine (Baltimore)*, *82*, 203–215.

Sweeney, H. L., & Houdusse, A. (2010). Structural and functional insights into the Myosin motor mechanism. *Annu Rev Biophys*, *39*, 539–557.

Vicente-Manzanares, M., Ma, X., Adelstein, R. S., et al. (2009). Non-muscle myosin II takes centre stage in cell adhesion and migration. *Nat Rev Mol Cell Biol*, *10*, 778–790.